

Supporting Information

Simplify: A Mass Spectrometry Metabolomics Approach to Identify Additives and Synergists from Complex Mixtures

Lindsay K. Caesar¹, Sabina Nogo¹, Cassandra N. Naphen¹, and Nadja B. Cech^{1,*}

¹ *Department of Chemistry & Biochemistry, University of North Carolina Greensboro, Greensboro, NC 27402, United States*

Content

- Figure S1: Fractionation Scheme
- Experimental Protocol: chromatographic separation and isolation of compounds **1**, **4**, and **5**.
- Figure S2: Fragmentation patterns of dihydrotanshinone I (compound **2**).
- Figure S3: Fragmentation patterns of tanshinone IIA (compound **3**).
- Figure S4: Fragmentation patterns of sugiol (compound **5**).
- Table S1: NMR data for sugiol (compound **5**) in CDCl₃
- Figure S5: ¹H-NMR data for compound **5** (500 MHz, CDCl₃)
- Figure S6: ¹³C-NMR data for compound **5** (125 MHz, CDCl₃)
- Figure S7: HSQC data for compound **5** (500 MHz, CDCl₃)
- Figure S8: HMBC data for compound **5** (500 MHz, CDCl₃)
- Figure S9: ¹H-NMR data for compound **5** (500 MHz, DMSO-d₆)
- Figure S10: ¹H-NMR data for compound **1** (500 MHz, CDCl₃)
- Figure S11: ¹³C-NMR data for compound **1** (125 MHz, CDCl₃)
- Figure S12: Fragmentation patterns of cryptotanshinone (compound **1**)
- Figure S13: ¹H-NMR data for compound **4** (500 MHz, CDCl₃)
- Figure S14: Calibration curve of cryptotanshinone (compound **1**)
- Table S2: Complete list of chemical contaminants removed from analysis using hierarchical cluster analysis coupled to spectral variable inspection of triplicate injections.
- Figure S15: Predicted versus actual activities of sub-fractions simplified from synergistic fraction SM-3 measured at 10 µg/mL.
- Figure S16: Dose response curves for compounds **1**, **2**, **3**, and **5**.

*Corresponding author

email: nadja_cech@uncg.edu, tel: 336-324-5011, fax: 336-334-5402

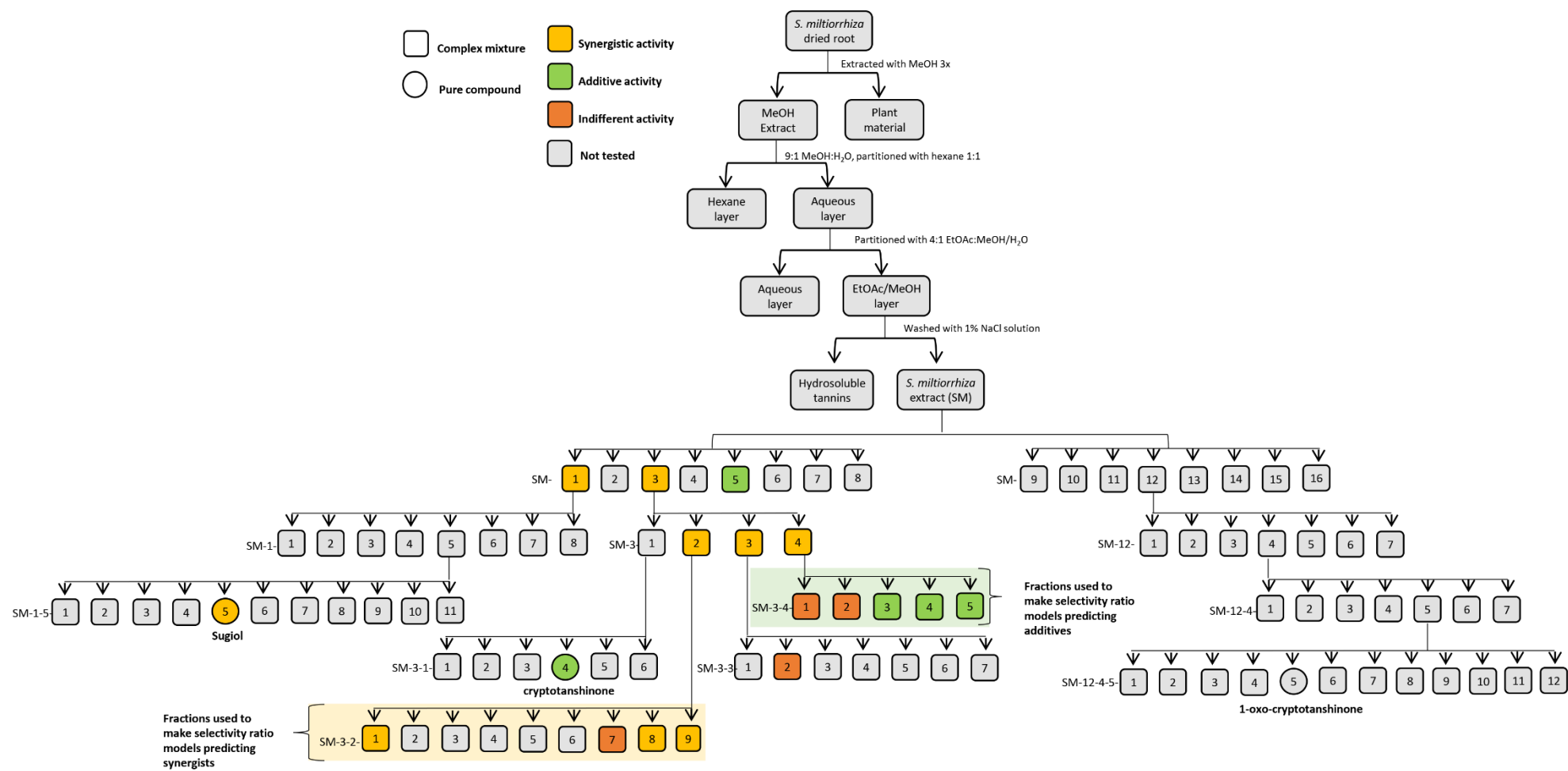


Figure S1: Fractionation Scheme

Experimental Protocol:

Materials and Methods

Chromatographic separation and isolation.

The first-stage separations of the EtOAc extract (SM) were conducted on an aliquot of 8.6 g of the extract using normal-stage flash chromatography (120-g silica column) at an 85 mL/min flow rate with a 45-min hexane/CH₃Cl/MeOH gradient. Two fractions, SM-1 and SM-3, were selected for further chromatographic separation. The first fraction (SM-1, 185.72 mg) was subjected to reversed-phase preparative HPLC injected onto a Gemini preparatory column (5 µm C18, 250 x 21.20 mm; Phenomenex) at a flow rate of 21.4 mL/min with a 45-min gradient. The gradient began at 65:35 CH₃CN:H₂O and increased to 90:10 over 35 min, following which the column was held at 100:0 for 10 min, yielding 8 fractions. Fraction 5 (SM-1-5, 36.51 mg) was subjected to a final round of reversed-phase preparative HPLC injected onto a Gemini preparatory column (5 µm C18, 250 x 21.20 mm; Phenomenex). The 30 min run began at 70:30 CH₃CN:H₂O and was increased to 100:0 over 30 min. Compound **5** (SM-1-5-5) eluted from 12-14 min (1.39 mg, 98% purity, 0.0003% yield). Fraction SM-3 (1058.67 mg) was subjected to a second round of normal-phase flash chromatography (40-g silica column) at a flow rate of 40 mL/min and a 55 min hexane/CH₃Cl/MeOH gradient, yielding four fractions. Fraction one (SM-3-1, 844.33 mg) eluted from 6-9 min, and was subjected to an additional round of reversed-phase flash chromatography using an 86g C18 reversed-phase RediSep Rf column with a 60 mL/min flow rate. A 60-min gradient of CH₃CN was used ranging from 45-100% CH₃CN. Compound **1** eluted at 25 min (580.01 mg, 95.0% purity, 0.1% yield).

Compound **4** was isolated using the remaining 9.7 g of the EtOAc extract (SM). First, normal-stage flash chromatography (80-g silica column) was conducted with a 40-min hexane/CH₃Cl/MeOH gradient and a 60 mL/min flow rate, yielding 8 fractions (SM-9 through SM-16). The fourth fraction, SM-12 (391.90 mg), was subjected to a second round of flash chromatography (12-g silica column, 30 mL/min) separated using a 45 gradient of hexane/EtOAc/MeOH. Of the seven resulting fractions (SM-12-1 through SM-12-7), the fourth fraction, SM-12-4 (108.01 mg), was fractionated using reversed-phase HPLC. The sample was injected onto a Gemini preparatory column (5 µm C18, 250 x 21.20 mm; Phenomenex) at a flow rate of 21.4 mL/min with a 45-min gradient. The gradient began at 40:60 CH₃CN:H₂O and increased to 50:50 over 35 min, after which the column was increased to 100:0 and held for 10 min, yielding 7 fractions (SM-12-4-1 through SM-12-4-7). Fraction SM-12-4-5 (3.19 mg) was purified with a final round of reversed-phase chromatography using a Gemini semi-preparatory column (5 µm C18, 250 x 10.00 mm; Phenomenex) at a flow rate of 4.7 mL/min and a 45-min gradient ranging from 43-48% CH₃CN. Compound **4** eluted at 18 min (0.5 mg, 93% purity, 0.0001% yield).

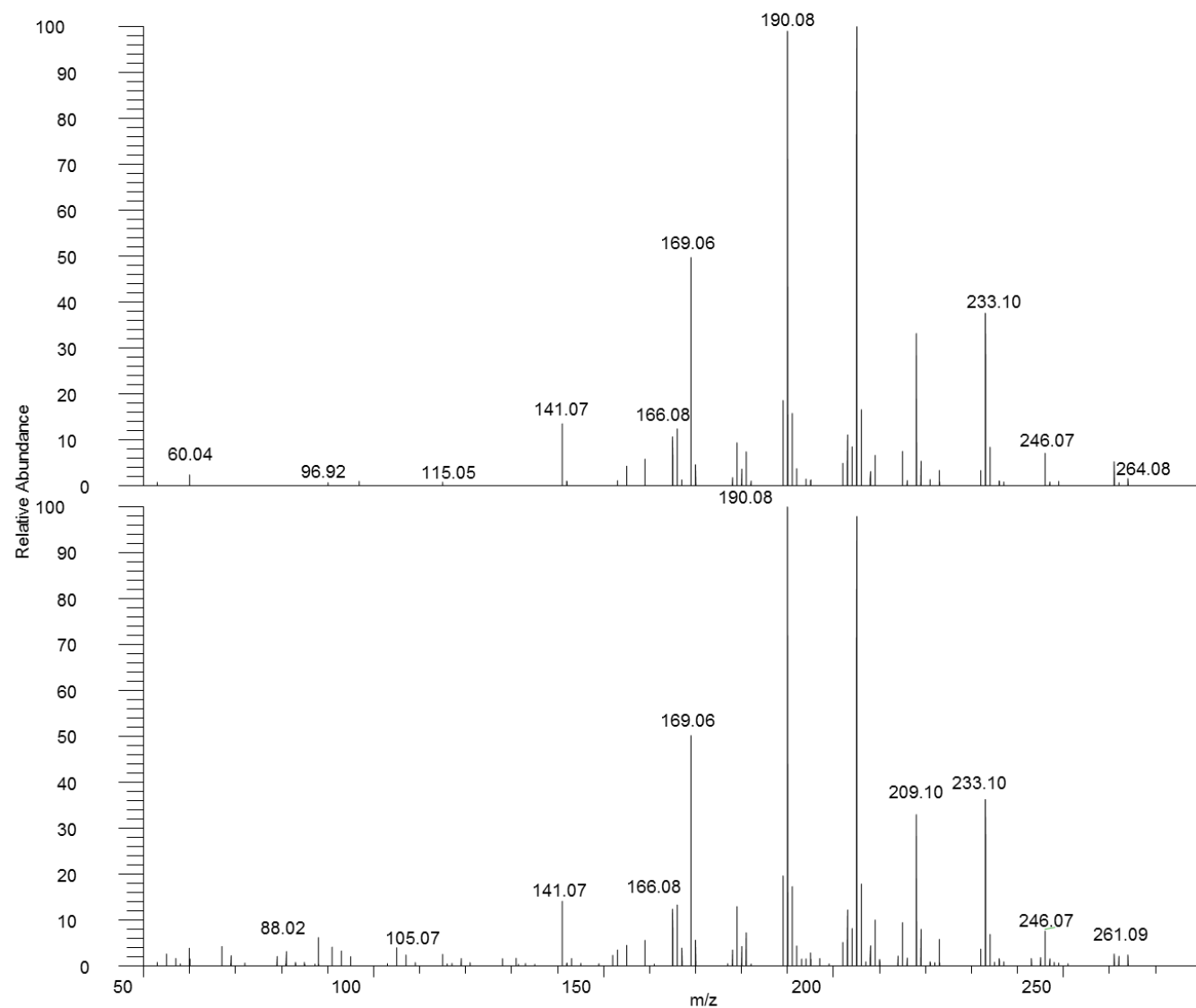


Figure S2. Fragmentation patterns of dihydrotanshinone I (compound **2**) fragmented with an HCD of 65. Fragmentation patterns of the pure standard compound (top) match fragmentation patterns of the compound found within the *S. miltiorrhiza* mixture (bottom).

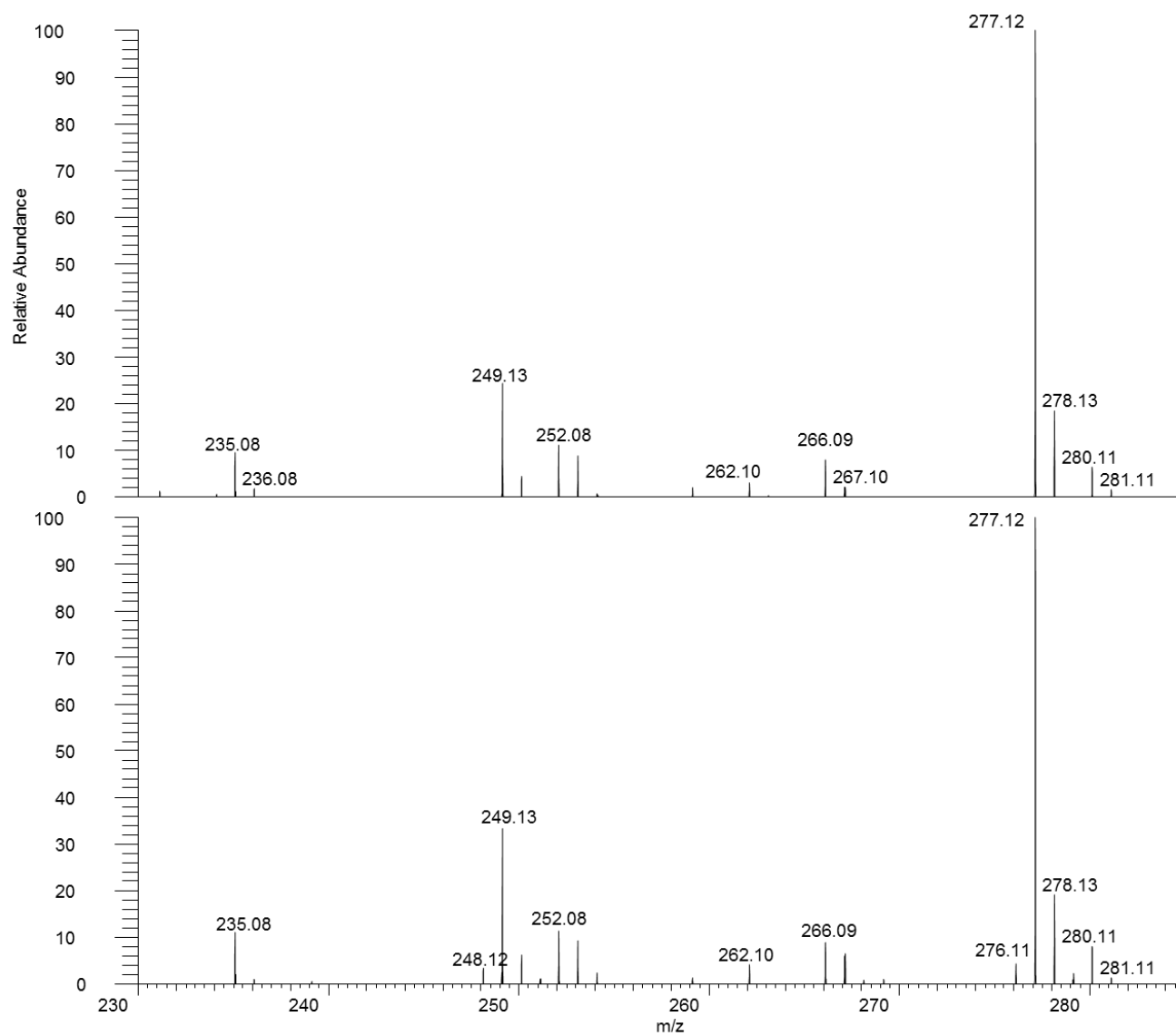


Figure S3. Fragmentation patterns of tanshinone IIA (compound **3**) fragmented with an HCD of 30. Fragmentation patterns of the pure standard compound (top) match fragmentation patterns of the compound found within the *S. miltiorrhiza* mixture (bottom).

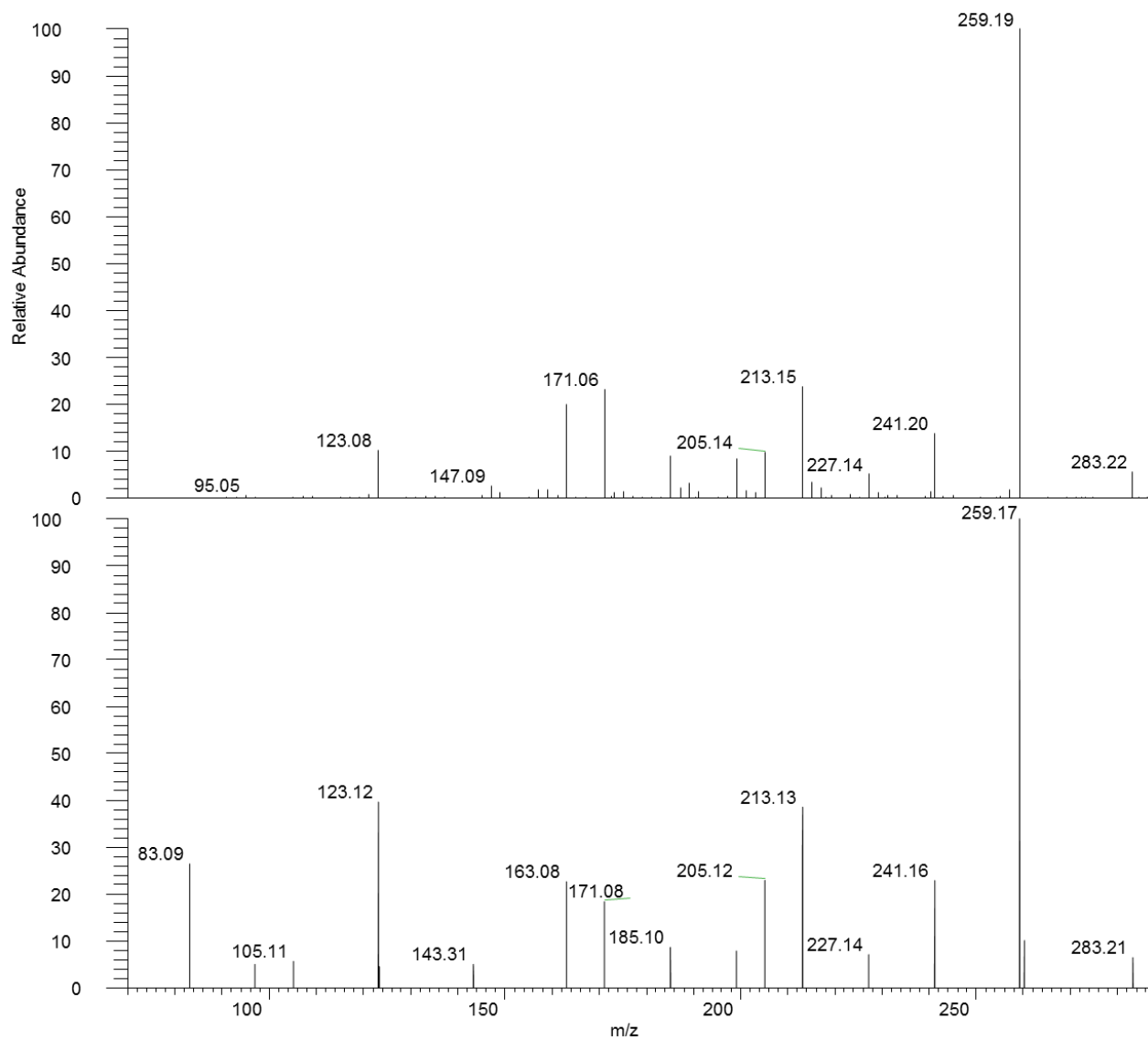
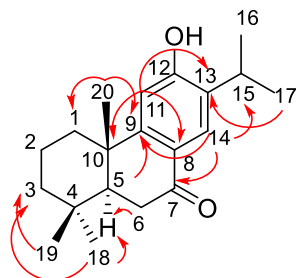


Figure S4. Fragmentation patterns of sugiol (compound **5**) fragmented with an HCD of 30. Fragmentation patterns of the purified compound (top) match fragmentation patterns of the compound found within the *S. miltiorrhiza* mixture (bottom).

Table S1: NMR data for sugiol (compound **5**) in CDCl₃, ¹H, HMBC, and HSQC data collected at 500 MHz, and ¹³C data collected at 125 MHz. Overlapping assignments (marked with an *) were determined using HSQC data in Figure S7. Key HMBC correlations have been illustrated on the chemical structure.



Position	¹³ C	¹ H	HMBC
1 α 1 β	37.97*	1.53 m* 2.23 dt (J=11.9, 2.8)	
2 α 2 β	18.97	1.67 m 1.76 tt (J=13.6, 3.3)	
3 α 3 β	41.42	1.25 m* 1.53 m*	
4	33.37		
5	49.53	1.85 dd (J=13.7, 4.0)	9
6 α 6 β	36.13	2.68 dd (J=18.1, 4.0) 2.58 dd (J=18.1, 13.8)	5
7	198.68		
8	124.78		
9	156.52		
10	37.95*		
11	110.03	6.68 s	10, 8, 13, 12
12	158.15		
13	132.63		
14	126.63	7.90 s	15, 9, 12, 7
15	26.88	3.12 hept (J=6.9)	
16	22.55	1.24 d (J=6.9)	13, 15, 17
17	22.42	1.26 d (J=6.9)	13, 16, 15
18	32.65	0.92 s	19, 3, 5
19	21.45	0.98 s	18, 3, 5
20	23.33	1.21 s	1, 5, 9

¹H NMR, 500 MHz, CDCl₃

	1H	type, J
18	0.92	3H, s
19	0.98	3H, s
20	1.21	3H, s
16	1.24	3H, d, J=6.9
3 α	1.25*	1H, m
17	1.26	3H, d, J=6.9
1 α	1.53*	1H, m
3 β	1.53*	1H, m
2 α	1.67	1H, m
2 β	1.76	1H, tt, J=13.6, 3.3
5	1.85	1H, dd, J=13.7, 4.0
1 β	2.23	1H, dt, J=11.9, 2.8
6 β	2.58	1H, dd, J=18.1, 13.8
6 α	2.68	1H, dd, J=18.1, 4.0
15	3.12	1H, hept, J=6.9
11	6.68	1H, s
14	7.90	1H, s

*overlapping assignments based on HSQC experiments.

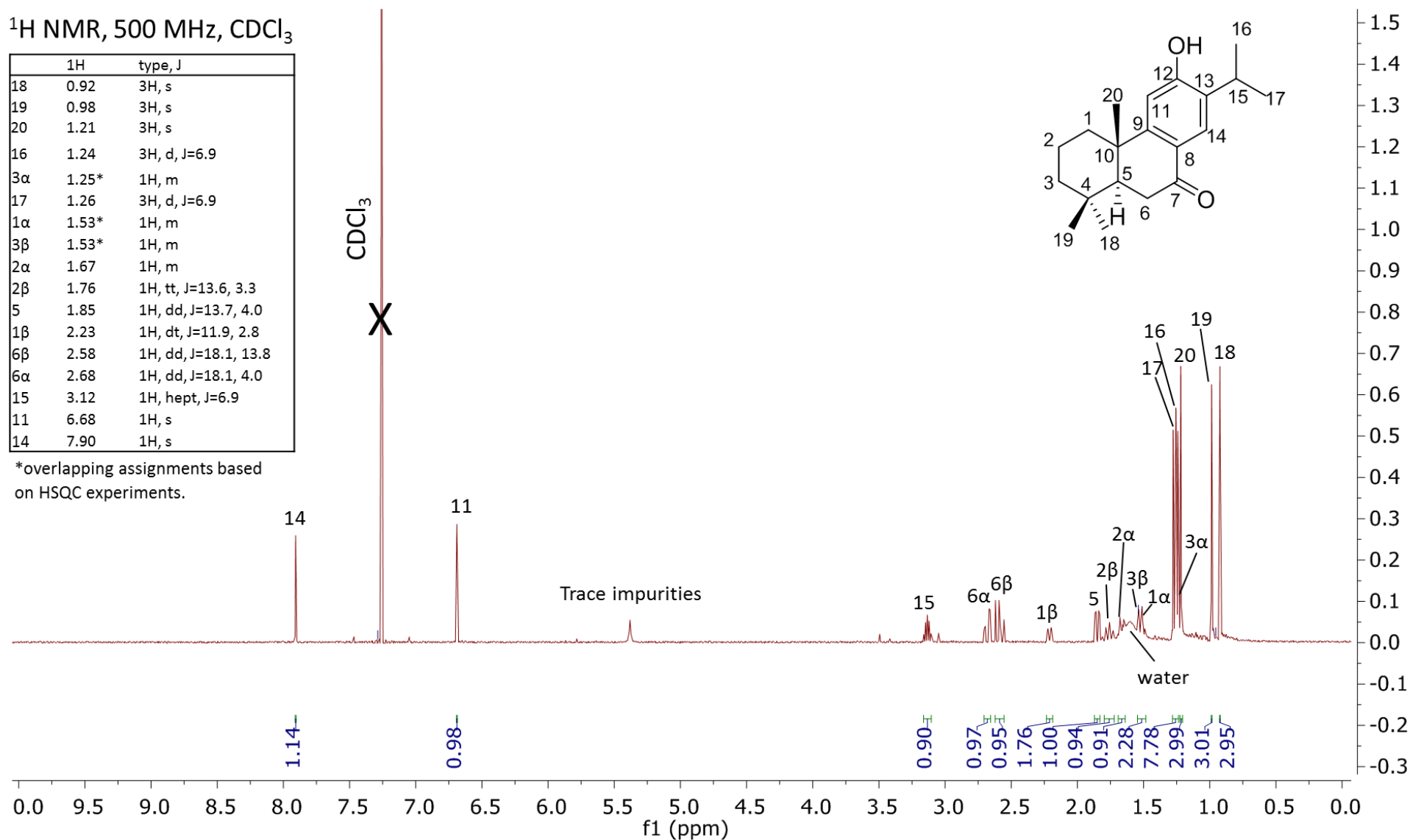


Figure S5. ¹H NMR data for compound **5** (500 MHz, CDCl₃).

^{13}C NMR, 125 MHz, CDCl_3

	^{13}C	Type
2	18.97	CH_2
19	21.45	CH_3
17	22.42	CH_3
16	22.55	CH_3
20	23.33	CH_3
15	26.88	CH
18	32.65	CH_3
4	33.37	C
6	36.13	CH_2
10	37.95*	C
1	37.97*	CH_2
3	41.42	CH_2
5	49.53	CH
11	110.03	CH
8	124.78	C
14	126.63	CH
13	132.63	C
9	156.52	C
12	158.15	C-OH
7	198.68	ketone

*overlapping assignments based on HSQC experiments.

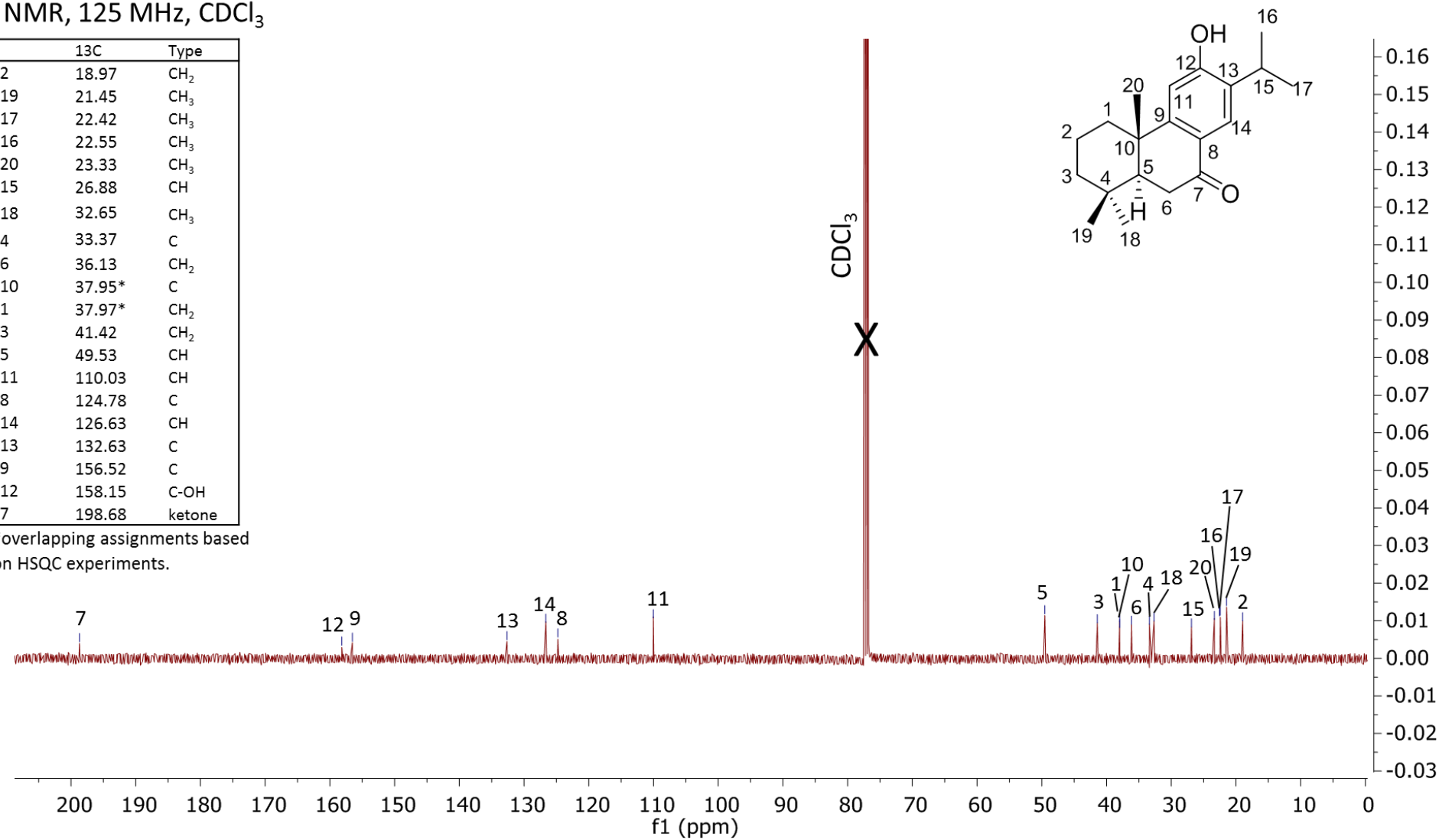


Figure S6. ^{13}C NMR data for compound **5** (125 MHz, CDCl_3).

HSQC, 500 MHz, CDCl_3

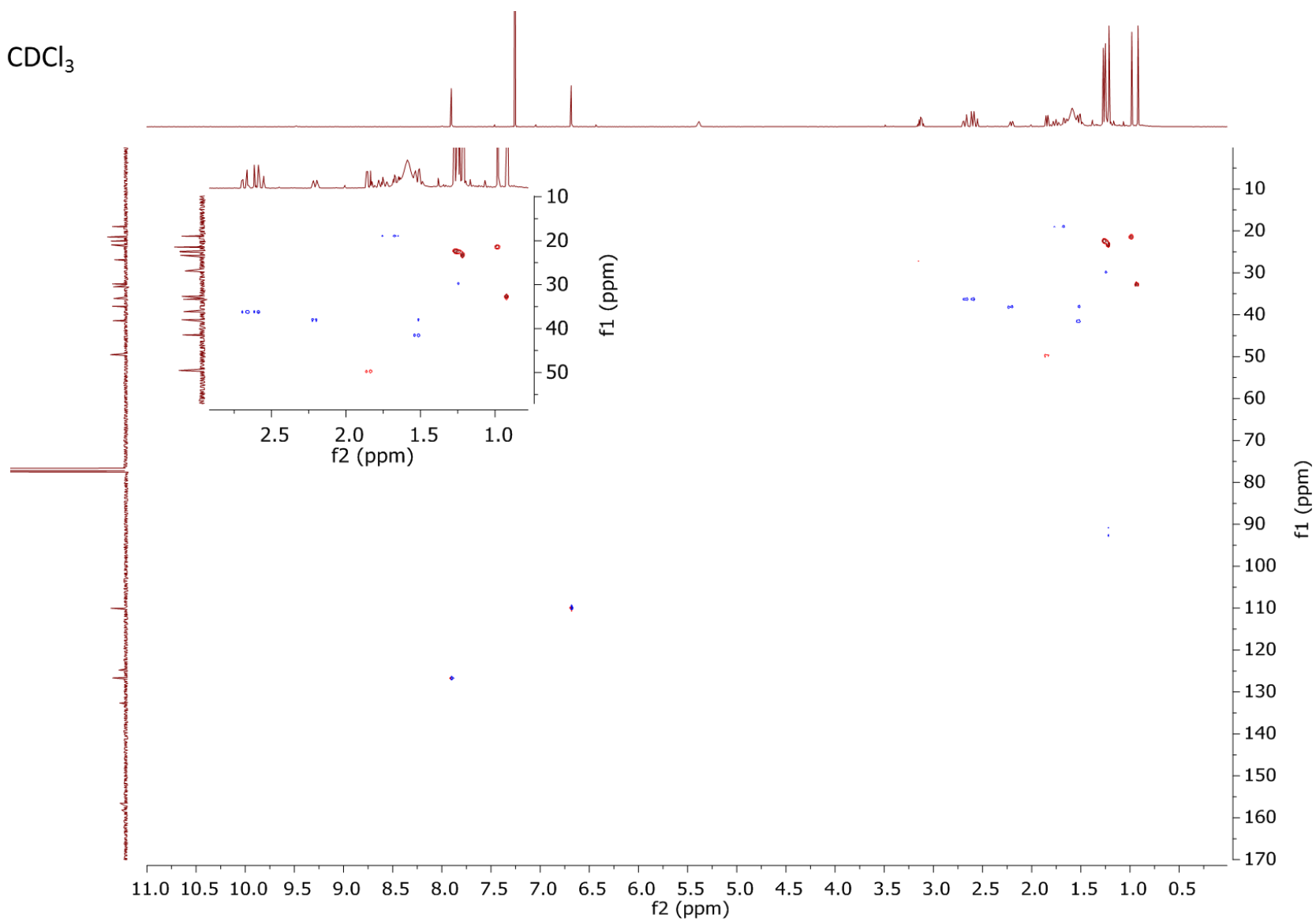


Figure S7. HSQC data for compound **5** (500 MHz, CDCl_3).

HMBC, 500 MHz, CDCl₃

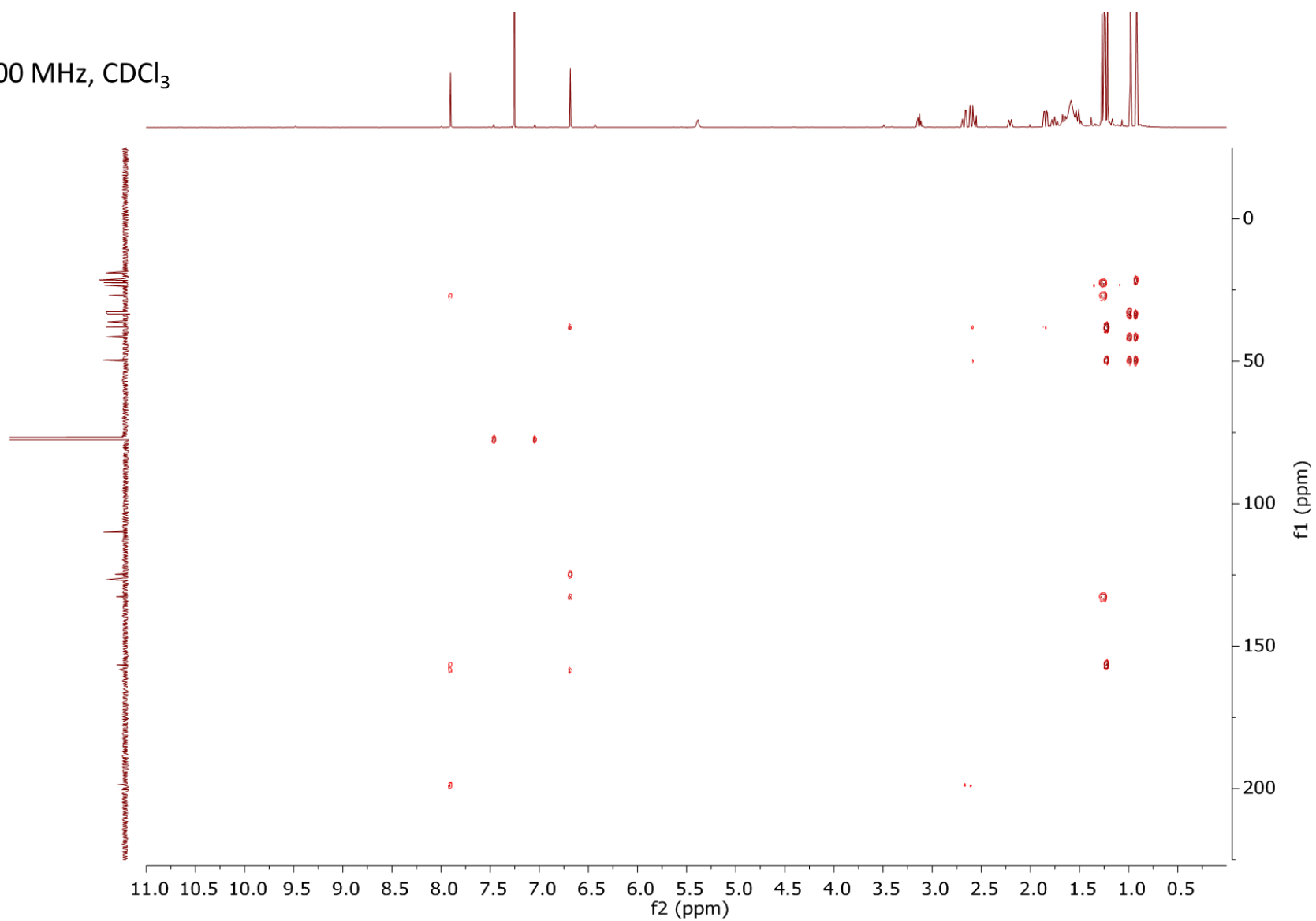


Figure S8. HMBC data for compound **5** (500 MHz, CDCl₃).

¹H NMR, 500 MHz, DMSO-d₆

	1H	type, J
18	0.88	3H, s
19	0.94	3H, s
16	1.12	3H, d, J=6.9
20	1.14	3H, s
17	1.15	3H, d, J=6.9
3α	1.19-1.61*	1H, m
1α	1.19-1.61*	1H, m
3β	1.19-1.61*	1H, m
2α	1.19-1.61*	1H, m
2β	1.19-1.61*	1H, m
5	1.73	1H, dd, J=13.7, 3.9
1β	2.13	1H, br d, J=12.3
6β	2.45	1H, dd, J=17.7, 3.8
6α	2.55	1H, dd, J=17.7, 13.6
15	3.13	1H hept, J=6.9
11	6.75	1H, s
14	7.63	1H, s

*overlapping peaks were not assigned specifically, but were assigned within a range, consistent with previous reports [1]

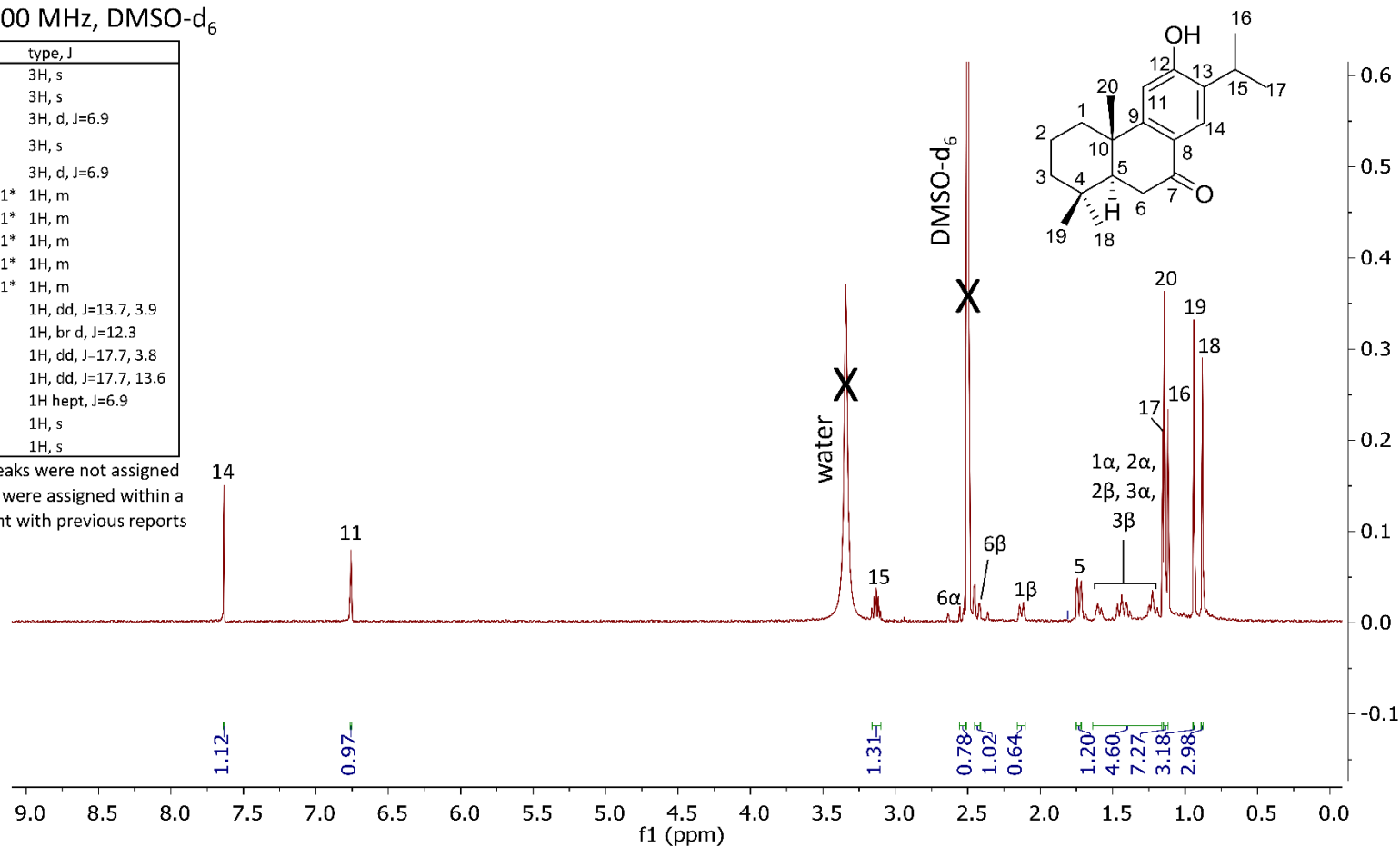


Figure S9. ¹H NMR data for compound **5** (500 MHz, DMSO-d₆). Data are consistent with previous reports.¹

^1H NMR, 500 MHz, CDCl_3

	^1H	type, J
18-19	1.29*	3H, s
	1.30*	3H, s
17	1.34	3H, d, J=6.8
2,3	1.64*	2H, m
	1.77*	2H, m
1	3.2	2H, t, J=6.4
15 α , 15 β , 16	3.59*	1H, dt, J=9.6, 6.4
	4.35*	1H, dd, J=9.3, 6.0
	4.88*	1H, t, J=9.5
6,7	7.48*	1H, d, J=8.1
	7.62*	1H, d, J=8.1

* Peaks were not assigned specifically between protons. All chemical shifts matched those reported in a previous study [2]

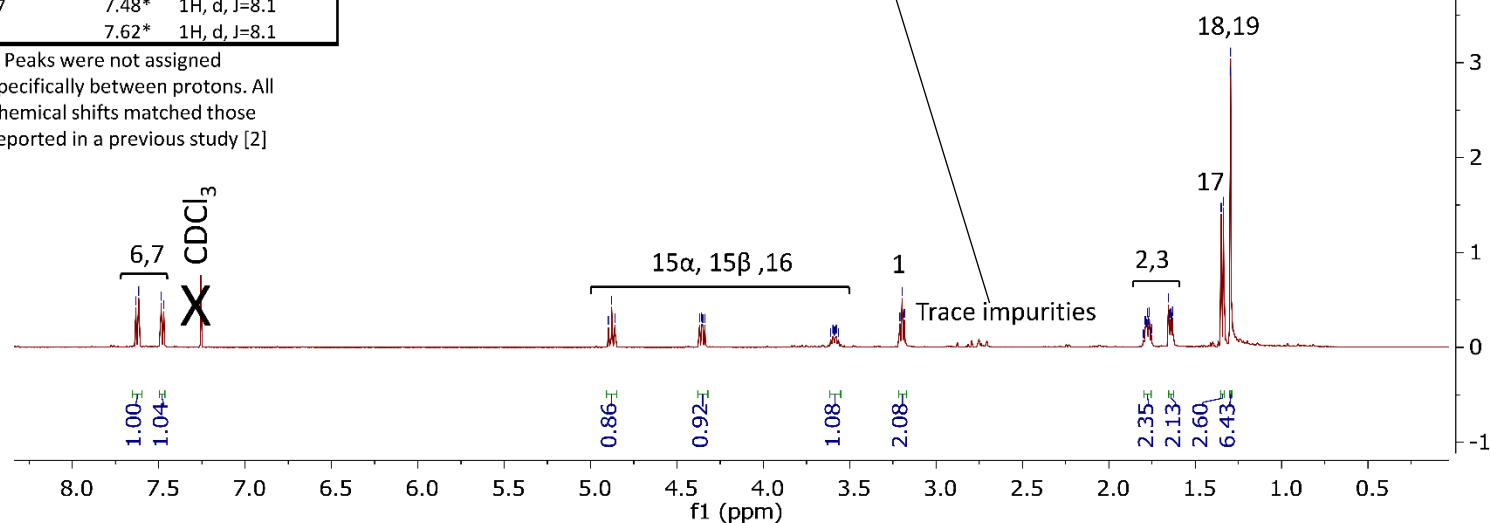
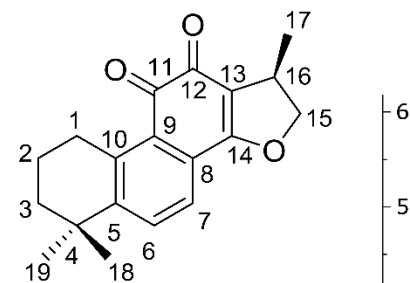
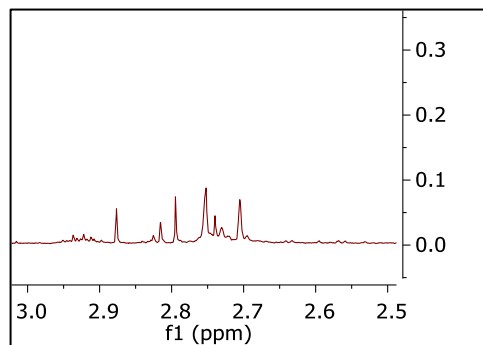


Figure S10. ^1H NMR data for compound **1** (500 MHz, CDCl_3). Data are consistent with previous reports.²

^{13}C NMR, 125 MHz, CDCl_3

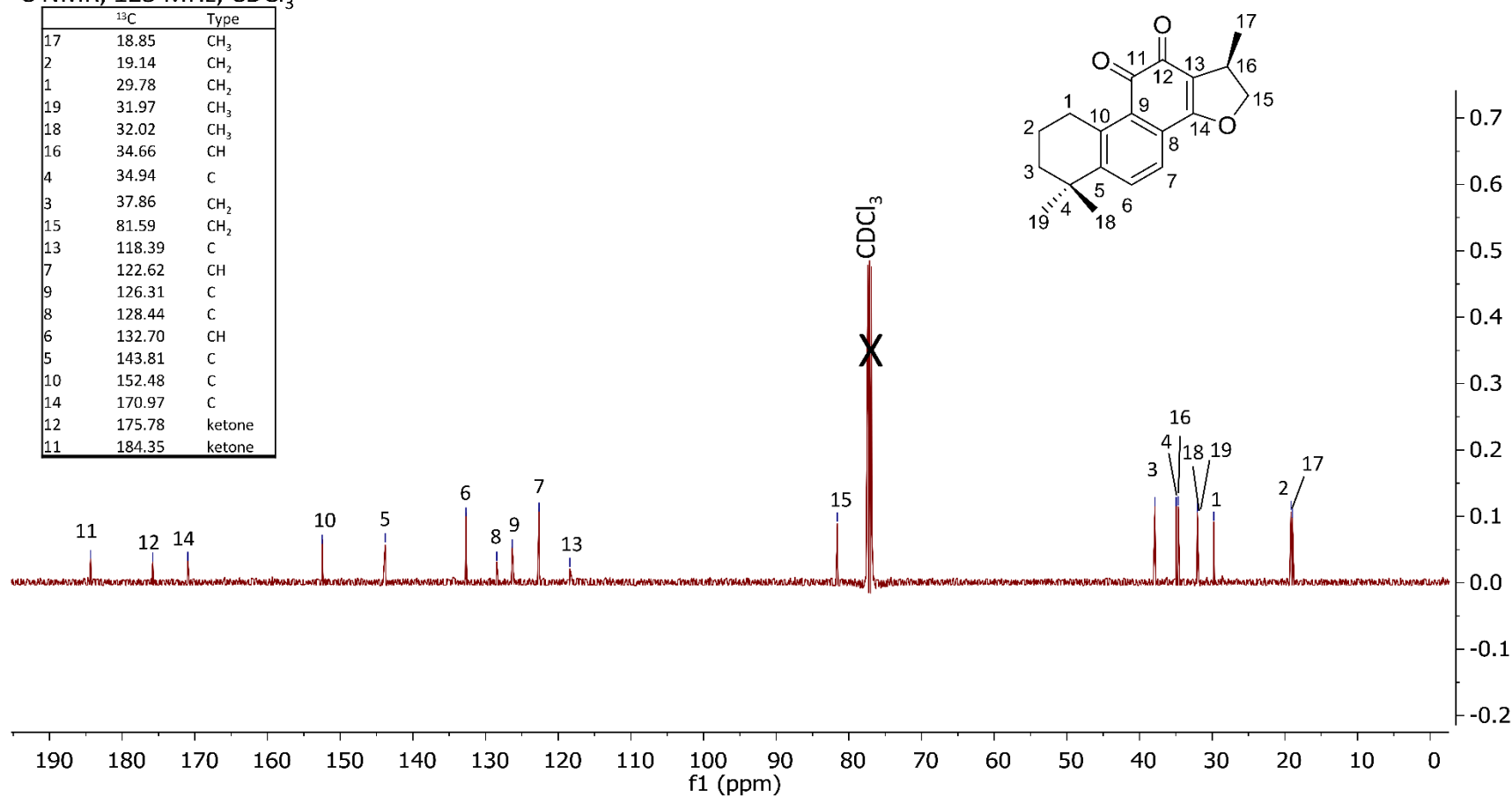


Figure S11. ^{13}C NMR data for compound **1** (125 MHz, CDCl_3). Traces are consistent with previous reports.²

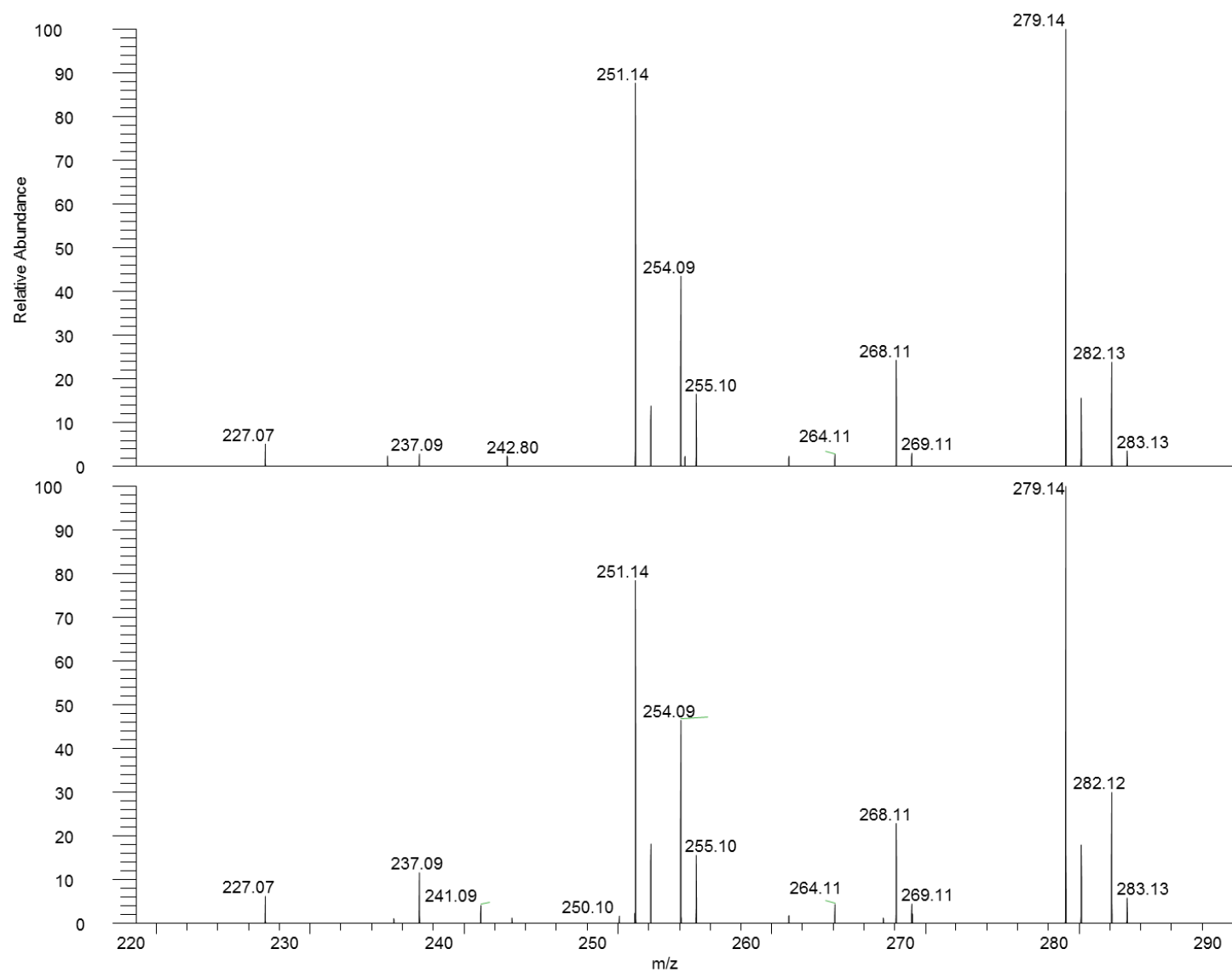


Figure S12. Fragmentation patterns of cryptotanshinone (compound **1**) fragmented with an HCD of 30. Fragmentation patterns of the pure standard compound (A) match fragmentation patterns of the compound isolated from the *S. miltiorrhiza* mixture (B).

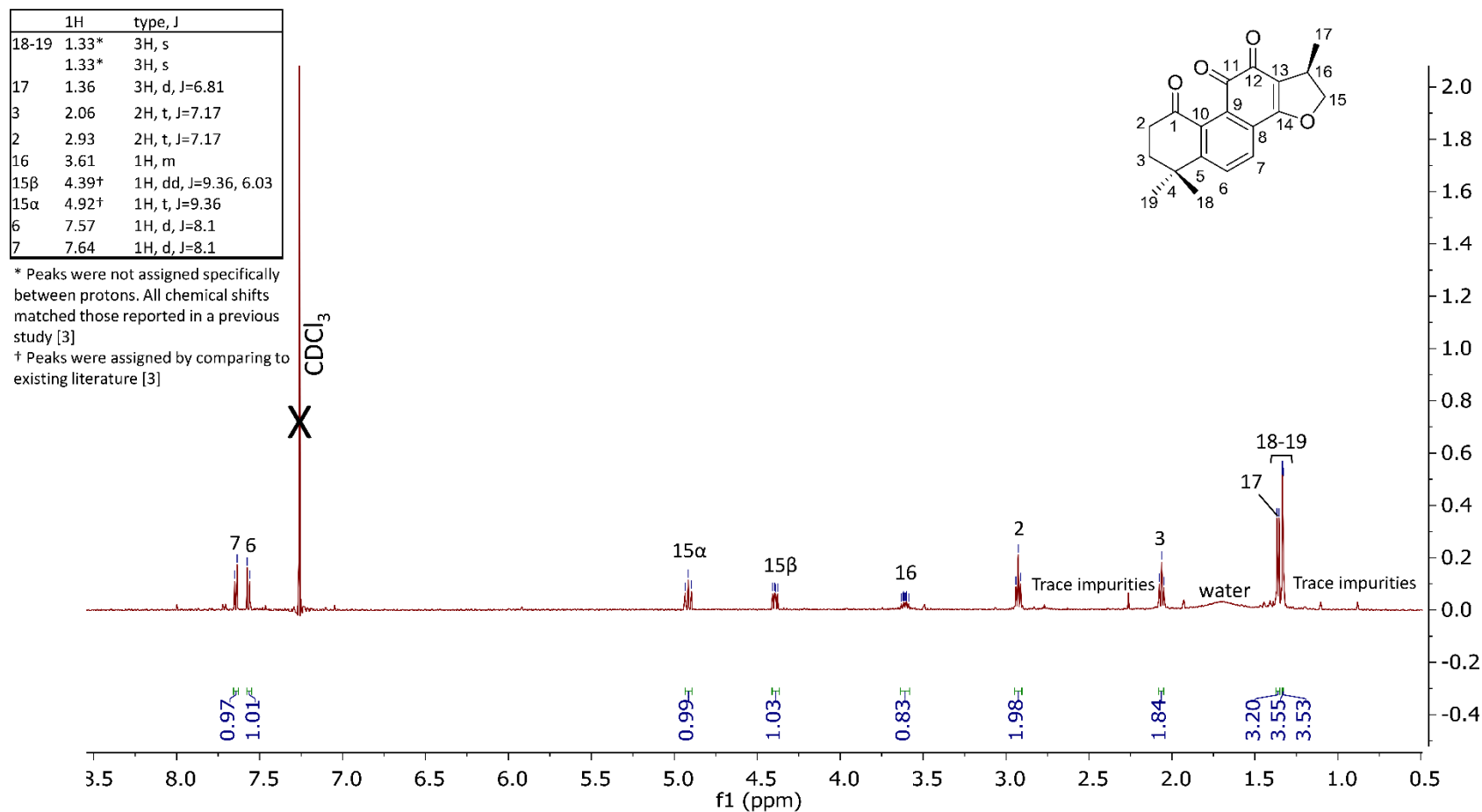


Figure S13: ¹H-NMR data for compound **4** (500 MHz, CDCl₃). Data are consistent with previous reports.³

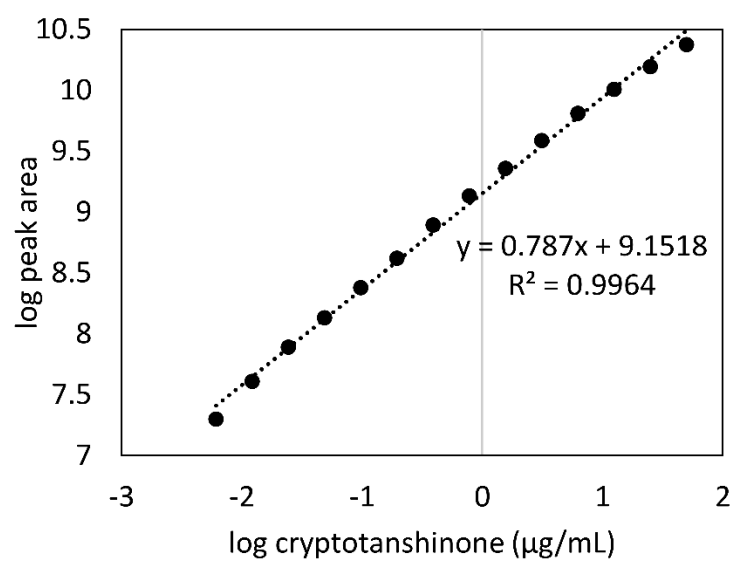


Figure S14. Calibration curve of cryptotanshinone used to quantify cryptotanshinone in each *S. miltiorrhiza* fraction.

Table S2: Complete list of chemical contaminants removed from analysis using hierarchical cluster analysis coupled to spectral variable inspection of triplicate injections. Chemical contaminants were consistent across samples.

Accurate Mass	Ionization Mode	Retention Time (min)	Tentative Identification*	Ion Type
279.159	Positive	8.66	Dibutylphthalate	[M+H] ⁺
336.636	Positive	5.88		
357.133	Negative	3.88		
357.133	Positive	4.04		
357.134	Negative	4.30		
357.134	Positive	4.70		
367.117	Positive	4.38		
536.166	Positive	8.55	Polysiloxane, [C ₂ H ₆ SiO] ₇	[M+NH ₄] ⁺
537.166	Positive	8.55	Polysiloxane, [C ₂ H ₆ SiO] ₇	[M+NH ₄] ⁺ , ¹³ C isotope
537.147†	Positive	8.56		
538.165	Positive	8.56	Polysiloxane, [C ₂ H ₆ SiO] ₇	[M+NH ₄] ⁺ , 2 × ¹³ C isotope
539.149 †	Positive	8.56		
539.165 †	Positive	8.55		
539.208	Positive	7.31		
540.161 †	Positive	8.55		
541.161 †	Positive	8.55		
837.216	Positive	8.97		
837.224	Positive	8.57		

* Tentative identifications accomplished using the following reference: Keller, B.O.; Sui, J.; Young, A.B.; Whittall, R.M. *Anal Chim Acta*. **2008**, 627(1), 71-81.⁴

† These masses represent peaks we believe to be associated with polysiloxane isotopes (containing more than 2 × ¹³C) and/or mass spectral artefacts. They were too low abundant to be fragmented using the LC-MS data analysis method, so they could not be confirmed to be the same as tentatively identified polysiloxanes. Instead, we have tentatively identified them by their similarity in accurate mass/retention time to putatively identified polysiloxanes from Keller et al.⁴

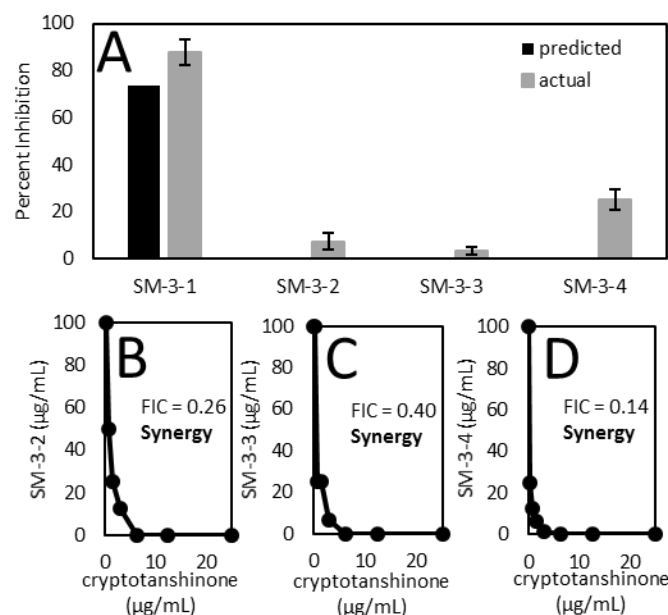


Figure S15A. Predicted versus actual activities of sub-fractions simplified from synergistic fraction SM-3 measured at 10 $\mu\text{g/mL}$. Although predicted and actual did not show a mismatch, we predicted that synergistic compounds were separated from cryptotanshinone which was used to calculate predicted activity. Cryptotanshinone was used as a positive control, and its MIC (25 $\mu\text{g/mL}$) is consistent with previous reports.⁵ Indeed, when isobolograms were generated for synergy testing, isobolograms of SM-3-2 (**B**), SM-3-3 (**C**), and SM-3-4 (**D**) all possessed synergy with FIC values of 0.26, 0.40, and 0.14 respectively.

FICs were calculated using the following equation: $[A]/IC_{50A} + [B]/IC_{50B} = \text{FIC}$, where IC_{50A} is the IC_{50} of cryptotanshinone alone, IC_{50B} is the IC_{50} of the fraction alone, $[A]$ is the IC_{50} of cryptotanshinone in combination with fraction, and $[B]$ is the IC_{50} of fraction in combination with cryptotanshinone. Synergy $\equiv \text{FIC} < 0.5$, additivity $\equiv 0.5 < \text{FIC} < 1.0$, Indifference $\equiv 1.0 < \text{FIC} < 4.0$ Antagonism $\equiv \text{FIC} > 4.0$.

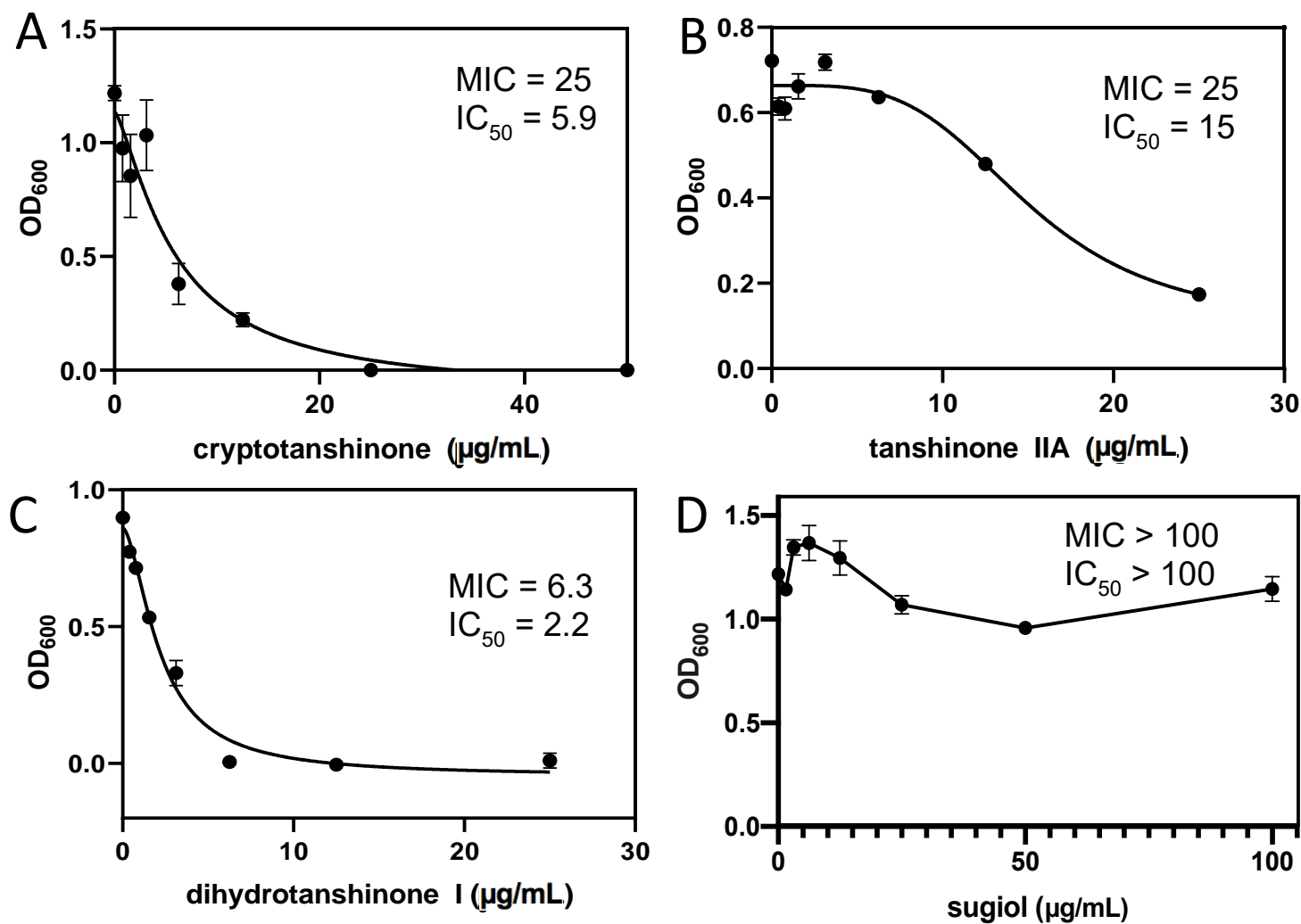


Figure S16. Dose response curves for cryptotanshinone (A), tanshinone IIA (B), dihydrotanshinone I (C), and sugiol (D). Curves were fit using a four-parameter logistic model in A-C. Sugiol, plotted in Figure S16D, did not possess antimicrobial activity, so a curve was not fit to this data.

REFERENCES

- [1] Li, A.; She, S.; Zhang, J.; Wu, T.; Pan, X. *Tetrahedron* **2003**, 59, 5737-5741.
- [2] Kang, H.S.; Chung, H.Y.; Jung, J.H.; Kang, S.S.; Choi, J.S. *Arch. Pharmacol Res.* **1997**, 20, 496.
- [3] Sairafianpour, M.; Christensen, J.; Staerk, D.; Budnik, B.A.; Kharazmi, A.; Bagherzadeh, K.; Jaroszewski, J.W. *J. Nat. Prod.* **2001**, 64, 1398-1403.
- [4] Keller, B.O.; Sui, J.; Young, A.B.; Whittal, R.M. *Anal. Chim. Acta* **2008**, 627, 71-81.
- [5] Lee, D.S.; Lee, S.H.; Noh, J.G.; Hong, S.D. *Biosci., Biotechnol., Biochem.* **1999**, 63, 2236-2239.